

# Observation of coherent $\pi^0$ electroproduction on deuterons at large momentum transfer

E. Tomasi-Gustafsson,<sup>1,2</sup> L. Bimbot,<sup>3</sup> S. Danagoulian,<sup>4,5</sup> K. Gustafsson,<sup>6</sup> D. Mack,<sup>5</sup>  
H. Mrktchyan,<sup>7</sup> and M. P. Rekalov<sup>1,8,9</sup>

<sup>1</sup>*LNS-Saclay, 91191 Gif-sur-Yvette, France*

<sup>2</sup>*DAPNIA/SPhN, CEA/Saclay, 91191 Gif-sur-Yvette, France*

<sup>3</sup>*IPNO, IN2P3, BP 1, 91406 Orsay, France*

<sup>4</sup>*North Carolina A. & T. State University, Greensboro, NC 27411, USA*

<sup>6</sup>*CERN/EP, CH-1211 Geneva 23, Switzerland*

<sup>5</sup>*Thomas Jefferson National Accelerator Facility, Newport News, VA 23606, USA*

<sup>7</sup>*Yerevan Physics Institute, 375036 Yerevan, Armenia*

<sup>8</sup>*Middle East Technical University, Physics Department, Ankara 06531, Turkey*

<sup>9</sup>*National Science Center: KFTI, 310108 Kharkov, Ukraine.*

## Abstract

The first experimental results for coherent  $\pi^0$ -electroproduction on the deuteron,  $e + d \rightarrow e + d + \pi^0$ , at large momentum transfer, are reported. The experiment was performed at Jefferson Laboratory at an incident electron energy of 4.05 GeV. A large pion production yield has been observed in a kinematical region for  $1.1 < Q^2 < 1.8$  GeV<sup>2</sup>, from threshold to 200 MeV excitation energy in the  $d\pi^0$  system. The  $Q^2$ -dependence is compared with theoretical predictions.

## I. INTRODUCTION

After elastic scattering, the reaction  $e + d \rightarrow e + d + \pi^0$  is the simplest coherent process for  $ed$ -collisions, which contains information on deuteron structure and on the elementary nucleon amplitudes. This reaction has characteristics which make it a very good source of knowledge on the deuteron structure, complementary to other probes. The presence of a deuteron with zero isospin in the initial and final states leads to a specific isotopic structure for the corresponding amplitudes. Elastic  $ed$ -scattering is essentially determined by an isoscalar combination of nucleon electromagnetic form factors, whereas coherent pion electroproduction on the deuteron allows a scan of the full isospin structure of the nucleon electromagnetic current in the resonance region and a separation of isoscalar and isovector contributions. This increases the degree of complexity, but simultaneously opens a unique way to progress in the understanding of the deuteron and nucleon structure.

Besides the calculation of static hadronic properties like masses or magnetic moments, the description of elastic and inelastic form factors (which contain dynamical information on hadron structure) represents a powerful test for theoretical models. In particular, in the intermediate energy region, the electromagnetic form factors should be a helpful signature of the transition from the confinement regime to perturbative QCD [1].

The experimental determination of the three form factors of the deuteron requires the measurement of polarization observables. The most recent elastic scattering  $ed$  data at large values of momentum transfer squared,  $Q^2 \leq 6 \text{ GeV}^2$  [2], have been successfully compared to pQCD predictions, whereas polarization measurements [3] lead to the conclusion that, up to  $Q^2 \simeq 2 \text{ GeV}^2$ , the deuteron structure can be described by conventional models based on nucleon and meson degrees of freedom. It seems very hard to extend such measurements to higher momentum transfer with existing techniques [4]. However, inelastic processes, such as  $e + d \rightarrow e + d + \pi^0$  (accessible with existing beams and polarimeters), probe the deuteron at smaller distances than in elastic scattering, for the same value of  $Q^2$ . An appropriate choice of kinematics can lead to new and interesting information. Two  $d\pi^0$ -excitation energy

regions seem particularly promising: the threshold region and the  $\Delta$ -excitation region.

A considerable experimental activity has been going on in the field of near threshold pion production in  $\gamma p$  collisions [5,6],  $ep$  collisions [7], and  $\gamma d$  collisions [8], but data on pion production in  $ed$  collisions are scarce. The experimental study of this reaction is now possible, at Mainz and at Jefferson Laboratory (JLab), due to the high duty cycle of the electron machines. Threshold  $\pi^0$ -electroproduction on protons and deuterons has been investigated by the A1-collaboration at Mainz [9] at small momentum transfer squared  $Q^2 \leq 0.1 \text{ GeV}^2$ .

At this low momentum transfer different nonperturbative QCD approaches, in particular Chiral Perturbation Theory (ChPT), can be applied. Phenomenological approaches such as effective Lagrangians models, isobar models, quark models, and hybrid models are widely applicable. A general theoretical study of pion electroproduction on deuterons was firstly developed in Ref. [10]. An adequate dynamical approach to pion electroproduction has to take into account all previous theoretical findings related to other electromagnetic processes on the deuteron, such as elastic  $ed$  scattering,  $\pi^0$ -photoproduction  $\gamma + d \rightarrow d + \pi^0$  [11], and deuteron photodisintegration  $\gamma + d \rightarrow n + p$  [12]. Like these processes, the reaction  $e + d \rightarrow e + d + \pi^0$  involves the study of the deuteron structure and of the reaction mechanism, and the determination of the neutron elementary amplitudes,  $\gamma^* + n \rightarrow n + \pi^0$ , where  $\gamma^*$  is a virtual photon. Note that the exact cancellation of rescattering effects, due to the processes:  $\gamma^* + d \rightarrow p + p + \pi^- (n + n + \pi^+) \rightarrow d\pi^0$  in the near threshold region [13], allows to extract the neutron amplitudes from the data about  $e + d \rightarrow e + d + \pi^0$ , in the frame of impulse approximation.

Here the first experimental observation of  $\pi^0$ -electroproduction on deuterons at large values of the momentum transfer squared and at relatively small excitation energy of the produced  $d\pi^0$ -system is reported. This kinematical region is only accessible at JLab.

The data were collected during the  $t_{20}$ -experiment, the primary aim of which was the measurement of the deuteron tensor polarization in elastic  $ed$ -scattering [3]. We have reconstructed the dependence on the kinematical variables which contain the physical information for the process  $e + d \rightarrow e + d + \pi^0$ , taking into account the difficulties related to limited ex-

perimental acceptance and to low detection efficiency. With a complete measurement of the five-fold differential cross section, the comparison to the theory would have been straightforward. Here the detection of the deuteron, due to limited resolution and statistics, does not allow a complete and precise reconstruction of the physical event. We derive from the experiment the  $Q^2$ -dependence of the yield, which can be directly compared to theoretical models, such as an effective Lagrangian model and pQCD predictions.

Our paper is organized as follows. In Section II we present kinematical and dynamical characteristics of the process  $e + d \rightarrow e + d + \pi^0$ . The description of the experiment is presented in Section III. Section IV is devoted to the discussion of the experimental results and to the comparison with theoretical predictions. The main results are summarized in the Conclusion. The Appendix contains a detailed scheme of the experimental analysis, in case of uncomplete event reconstruction.

## II. THE PROCESS $e + d \rightarrow e + d + \pi^0$

### A. The kinematics

In the framework of the one photon mechanism, the process  $e + d \rightarrow e + X$  is equivalent to  $\gamma^* + d \rightarrow X$ , where  $X$  is a hadronic system, and this gives the most convenient choice of kinematical variables for the electroproduction processes. The detection of the recoil deuteron in coincidence with the scattered electron allows a full reconstruction of the kinematics for  $\gamma^* + d \rightarrow d + \pi^0$ .

In the limit of zero electron mass, the momentum transfer squared from the incident to the outgoing electron,  $Q^2$ , is defined as

$$Q^2 = 4E_1 E_2 \sin^2 \frac{\theta_e}{2},$$

where  $E_1$ , ( $E_2$ ) is the energy of the incident (scattered) electron and  $\theta_e$  is the electron scattering angle (in the LAB-system). As defined here,  $Q^2$  is positive in the space-like region.

The energy and the angle of the scattered electron enable the determination of the momentum transfer squared,  $Q^2$ , and of the invariant mass of the produced hadronic system,  $W$ :

$$W = \sqrt{M^2 - Q^2 + 2\nu^*},$$

where  $M$  is the deuteron mass and the quantity  $\nu^* = M(E_1 - E_2)$  is related to the energy transferred from the electron to the hadronic system  $X$ .

Events from elastic scattering and electroproduction of one and two pions follow straight lines in a plane defined by  $Q^2$  versus  $\nu^*$  (Fig. 1), corresponding to a definite value of the invariant mass  $W$ . Fixed values of  $\theta_e$  correspond also to straight lines in the  $Q^2$ - $\nu^*$  plane. In Fig. 1 the lines corresponding to  $\theta_e = 18.5^\circ(\pm 1.5^\circ)$ , are drawn to emphasize the kinematical limits of the experimental set-up.

For the analysis of the  $\pi^0$  production data near threshold, instead of the invariant variable  $t = (p_1 - p_2)^2$  ( $p_1$  and  $p_2$  are the four-momenta of the target and of the outgoing deuteron, respectively), it is preferable to use  $\cos\tilde{\theta}_\pi$ , where  $\tilde{\theta}_\pi$  is the pion production angle in the center of mass system (CMS) of the final  $d\pi^0$ -system .

At a given value of  $W$ , the final deuteron energy in the laboratory system,  $E_d$ , can be expressed as a quadratic function of the cosine of the deuteron scattering angle,  $\cos\theta_d$ , which is drawn in Fig. 2 for different values of  $W$ . In this figure the threshold point for  $\pi^0$  electroproduction and the point for elastic  $ed$  kinematics, at a fixed value of incident electron energy and electron scattering angle, are also indicated.

These considerations are valid for coplanar kinematics, where all momenta of the final particles in  $e + d \rightarrow e + d + \pi^0$  are in the same plane. This corresponds to two values of the azimuthal angle of the final deuteron,  $\phi = 0$  and  $\phi = \pi$ , relative to the electron scattering plane, defined by the directions of the three-momenta of the initial and final electrons  $\vec{k}_1$  and  $\vec{k}_2$ . The left-hand side of each ellipse in Fig. 2 (with respect to the center, i.e. the threshold point) corresponds to  $\phi = \pi$  (the deuteron scattering angle is smaller than the threshold value) and the right-hand side of the ellipses corresponds to  $\phi = 0$  (the deuteron

scattering angle is larger than the threshold value).

Note, in conclusion, that the measurement of  $E_d$  allows the determination of  $\cos \tilde{\theta}_\pi$  as a function of  $E_d$ ,  $W$ , and  $Q^2$  through the following expression:

$$2M^2 - 2ME_d = -Q^2 + m_\pi^2 - \frac{(W^2 - Q^2 - M^2)(W^2 + m_\pi^2 - M^2)}{2W^2} \quad (1)$$

$$+ 2\cos\tilde{\theta}_\pi \sqrt{\left[\frac{(W^2 - Q^2 - M^2)^2}{4W^2} + Q^2\right] \left[\frac{(W^2 + m_\pi^2 - M^2)^2}{4W^2} - m_\pi^2\right]}.$$

The knowledge of the  $\cos \tilde{\theta}_\pi$ -dependence for the differential cross section of  $\gamma^* + d \rightarrow d + \pi^0$ , is essential in order to perform a multipole analysis.

## B. The dynamics

In the framework of the one-photon mechanism, the differential cross section for  $e + d \rightarrow e + d + \pi^0$ , can be written as [14]:

$$\sigma(\phi) = \frac{d^5\sigma}{dE_2 d\Omega d\tilde{\Omega}} = \mathcal{N} \left[ \mathcal{H}_T + \epsilon \mathcal{H}_L + \epsilon \mathcal{H}_P \cos 2\phi + \sqrt{2\epsilon(1+\epsilon)} \mathcal{H}_I \cos \phi \right], \quad (2)$$

where  $\mathcal{N}$  is a normalization kinematical coefficient:

$$\mathcal{N} = \frac{\alpha^2 E_2 q_\pi}{64\pi^3 E_1 MW} \frac{1}{(1-\epsilon) Q^2}, \quad (3)$$

and  $\epsilon$  is the degree of linear polarization of the virtual photon:

$$\epsilon^{-1} = 1 + 2 \frac{\vec{k}_\gamma^2}{Q^2} \tan^2 \frac{\theta_e}{2}, \quad (4)$$

Here  $\vec{k}_\gamma^2 = (\vec{k}_1 - \vec{k}_2)^2 = E_1^2 + E_2^2 - 2E_1 E_2 \cos \theta_e$ ,  $\vec{q}_\pi$  is the pion three-momentum in the CMS of the reaction  $\gamma^* + d \rightarrow d + \pi^0$  with  $q_\pi^2 = E_\pi^2 - m_\pi^2$ ,  $E_\pi = \frac{W^2 + m_\pi^2 - M^2}{2W}$ , and  $\alpha = \frac{e^2}{4\pi} \simeq \frac{1}{137}$ .

The terms  $\mathcal{H}_a$  ( $a = T, L, P, I$ ), are related to the four standard contributions to the differential cross section for  $\gamma^* + d \rightarrow d + \pi^0$ , corresponding to the different polarizations of the virtual photon:  $T, P$  are the transverse components,  $L$  is the longitudinal component and  $I$  is the interference between the longitudinal and the transversal components. The element of solid angle for the scattered electron (deuteron) in the LAB (CMS) system is  $d\Omega$  ( $d\tilde{\Omega}$ ). Note that  $d\tilde{\Omega} = d \cos \tilde{\theta}_\pi d\phi_\pi$ .

The different contributions  $\mathcal{H}_a$  depend on  $Q^2$ ,  $W$ , and  $\cos \tilde{\theta}_\pi$ . The azimuthal dependence is explicit in the cosine terms, Eq. (2). The three kinematical quantities  $\epsilon$ ,  $\mathcal{N}$  and  $\phi$  depend on the electron kinematics.

A measurement of  $\sigma(\phi)$  for 3 values of  $\phi$  (for example  $\phi = 0$ ,  $\pi/2$ , and  $\pi$ ) and for two values of the parameter  $\epsilon$  allows a complete and unique separation of all the four contributions to the cross section. Note that Eq. (2) can be considered a generalization of the Rosenbluth formula for a three-body reaction, in which only two particles are detected in the final state.

In the near threshold region, in the framework of the S- and P-waves pion production, the four contributions to the differential cross section of  $e + d \rightarrow e + d + \pi^0$ , can be parameterized as the functions of  $\cos \tilde{\theta}_\pi$  as follows (omitting, for simplicity, the deuteron form factors):

$$\begin{aligned} \mathcal{H}_T &= a_0 + a_1 \cos \tilde{\theta}_\pi + a_2 \cos^2 \tilde{\theta}_\pi, & \mathcal{H}_P &= b_0 \sin^2 \tilde{\theta}_\pi, \\ \mathcal{H}_L &= c_0 + c_1 \cos \tilde{\theta}_\pi + c_2 \cos^2 \tilde{\theta}_\pi, & \mathcal{H}_I &= \sin \tilde{\theta}_\pi (d_0 + d_1 \cos \tilde{\theta}_\pi), \end{aligned} \quad (5)$$

where the real coefficients  $a_i$ ,  $b_i$ ,  $c_i$ , and  $d_i$  are well defined quadratic combinations of multipole amplitudes for  $\gamma^* + d \rightarrow d + \pi^0$ , which are functions of only two variables,  $Q^2$  and  $W$ . All the dynamical information about this process is contained in these multipole amplitudes. The experimental determination of the  $Q^2$  and  $W$  dependences of the multipole amplitudes would allow a direct comparison with the theory. In the framework of the S- and P-wave contributions, the five-fold cross section has to be measured for at least nine points (for different  $\cos \tilde{\theta}_\pi$ ,  $\phi$ , and  $\epsilon$ ) in order to fully determine the multipole amplitudes (the moduli and relative phases).

In the case of limited acceptance or of partial information on one or both of the final particles, one can extract from the experiment - and compare to theoretical predictions - only some combinations of the above mentioned coefficients. For example, near threshold, the pions are emitted in a narrow cone around the virtual photon direction (in the LAB system) and the experimental resolution may not allow a precise determination of the azimuthal angle, or, on the contrary, far above threshold, the detection acceptance may not cover the

full phase space. We detail in the Appendix, a rigorous method for the data analysis, in case of limited kinematical information.

### III. THE EXPERIMENT

From Figs. 1 and 2, it appears that the kinematical characteristics of the outgoing particles (the scattered electron and deuteron) in the process  $e + d \rightarrow e + d + \pi^0$  in the threshold region, are near to those of the elastic process  $e + d \rightarrow e + d$ . Therefore the experimental set up of the  $t_{20}$  experiment at JLab, which had a double arm detection for elastic  $ed$  scattering, could be used to study the inelastic process of  $\pi^0$ -production. The experiment was performed in Hall C. With small changes in the spectrometer settings, it was possible to reach near threshold kinematics in which  $\pi^0$  events were detected. The typical luminosity was about  $2 \cdot 10^{38} \text{ cm}^2\text{s}^{-1}$  obtained with a  $40 \mu\text{A}$  continuous electron beam and a 12 cm long liquid deuterium target. The electrons were detected in a large solid angle (6 msr) spectrometer (HMS) with an energy resolution  $\Delta E/E = 10^{-3}$ . The deuterons were focussed on the polarimeter POLDER [15] through a magnetic transport line located at a fixed angle,  $\theta_d$ , of  $60.5^\circ$ . For the initial electron energy,  $E_e = 4.05 \text{ GeV}$ , the scattered electrons were detected at an angle  $\theta_e = 18.5^\circ$  corresponding to a range of four momentum squared  $1.1 < Q^2 < 1.8 \text{ GeV}^2$ . The coincidence between electrons and deuterons reduced the high background. A more detailed description of the experimental set up can be found in [3,16].

The deuterons were identified in the two-dimensional spectrum corresponding to time of flight versus the ADC signal related to the energy loss in the POLDER start detectors. The deuterons were selected by the contour shown in Fig. 3 (contour I, labelled 'signal'). An estimation of the background, done by displacing the contour (contour II, labelled 'background'), is about 20%. The largest part of the background, corresponding to protons coming from deuteron break up does not appear on the figure, as it corresponds to a different region of the time of flight spectrum.



The spectrum of the invariant mass  $W$  is shown in Fig. 4 for different selection criteria of events. Above the pion threshold,  $W_{th} = M + m_\pi$ , a significant number of events were observed. The transition between the elastic and the pion production regions is illustrated in Figs. 5 and 6. The number of counts is plotted as a two-dimensional function of  $Q^2$  and  $W$ , for the  $e + d \rightarrow e + X$  reaction, for spectrometer settings corresponding to elastic kinematics (Fig. 5) and to pion kinematics (Fig. 6), where a tail from elastic scattering is still visible. The experimental resolutions are  $\frac{\Delta W}{W} = 0.3\%$  and  $\frac{\Delta Q^2}{Q^2} = 0.7\%$ .

In this measurement, in four hours beam on target, 25815 pion events were counted in contour I, 330 of which correspond to the near threshold region in an invariant mass range  $\Delta W = W - W_{th} = 40$  MeV. This total number is comparable to the number of events for elastic  $ed$ -scattering in similar experimental conditions.

#### IV. THE RESULTS

The deuteron magnetic channel has large angular acceptance and low momentum resolution. The deuteron momentum and scattering angle could not be reconstructed with precision. For this reason the information presented here concerns the kinematical variables calculated from the electron channel. We focus here on the  $Q^2$ -dependence of the differential cross section of the process  $e + d \rightarrow e + d + \pi^0$ , for which theoretical predictions are available.

In Fig. 7 we show the Monte Carlo expectation [17] for the  $Q^2$  and the  $W$ -distributions, calculated for a uniform input distribution (solid line) and for a distribution weighted by the kinematical factor  $\mathcal{N}$  (Eq. 3). The figure shows the range of detection, where the acceptance of the apparatus is reasonably flat:  $1.3 \leq Q^2 \leq 1.6$  GeV<sup>2</sup> and  $W$  from threshold up to 2.3 GeV.

In order to extract the  $Q^2$ -distribution, quite conservative cuts were applied in order to select events well inside the acceptance of the deuteron channel. We assumed that the efficiency is constant in this central region. This is reasonably supported by the Monte Carlo simulations.

Systematic errors due to event selection were estimated with the help of a parallel analysis, where the selection of events was done by a window in the time of flight and electron momentum bi-dimensional plot. Background subtraction was done by displacing a window in the time of flight spectrum. The final distributions were consistent within the error bars.

In Fig. 8 the  $Q^2$ -dependence of the counting rates integrated over the experimental acceptance, is given for different region of  $W$ , in bins of 40 MeV, from threshold to the  $\Delta$ -excitation region. The data are corrected by the kinematical factor  $\mathcal{N}$  (see Eq. 3) in order to make an easier comparison with the theoretical predictions. We did not attempt to apply an absolute normalization of the data due to a too large uncertainty on the reconstruction of the deuteron kinematics, although the  $d\pi^0$  events were unambiguously identified.

Moreover the radiative corrections are necessary to extract absolute values of the cross section. For the considered process, at relatively large momentum transfer, radiative corrections are, in principle, far from being negligible. Their calculation is complicated from a theoretical point of view, and at our knowledge, no calculation exists for pion coherent electroproduction on the deuteron. Furthermore, the acceptance has to be taken precisely into account. But, if we consider relative yields, this problem can be neglected, mainly due to the logarithmic, i.e. weak dependence of radiative corrections on  $Q^2$  and relatively small  $Q^2$ -interval in the present experiment.

The four spectra present a similar step decreasing behavior <sup>1</sup>. In general the acceptance in one variable is a complicated function of other variables and it is usually estimated through sophisticated simulations. But if the  $\phi$ -acceptance is small or constant, or in the case of full  $2\pi$   $\phi$ -acceptance, a rigorous treatment of the data is possible, even without full information on the azimuthal angle (see Appendix). The relative  $Q^2$ -dependence of the yields can be compared with theoretical calculations, such as impulse approximation or pQCD scaling

---

<sup>1</sup>The deviation from a monotonic decreasing for  $Q^2 \geq 1.6 \text{ GeV}^2$  may reflect a limitation in the acceptance (see Fig. 7).

laws [18].

Predictions available from a classical (mesonic) model on coherent pion electroproduction [10], where the reaction mechanism is described within the impulse approximation (the deuteron is described by the Paris wave function), and the  $\gamma^* + N \rightarrow N + \pi$ -interaction is treated in the framework of an effective Lagrangian model [10], are shown in Fig. 8. The solid and dashed lines correspond respectively to  $\phi$ -integration over  $2\pi$  and to the limit for small  $\Delta\phi$ , which is closer to the experimental conditions. For  $2\pi$ -acceptance only  $\mathcal{H}_T$  and  $\mathcal{H}_L$  contribute to the cross section, whereas, in the case of small  $\phi$ -acceptance, all contributions to the exclusive cross section are present (see Appendix).

The theoretical curves are normalized to the highest experimental point, for the smallest value of  $Q^2$ . After normalization, the results are not very sensitive to the opening of the azimuthal angle. Such behavior can be interpreted as an indication of a weak  $\phi$ -dependence of the  $d(e, e'\pi^0)d$  cross section. Another possibility is that the different contributions induce a similar  $Q^2$ -dependence of the cross section, integrated in this kinematical region. The theoretical model [10] predicts indeed a large  $\phi$ -dependence in the  $\Delta$ -region.

Following the quark counting rule of pQCD, [1], the asymptotic behaviour of the electromagnetic (elastic and inelastic) form factors of hadrons follows a  $(1/Q^2)^{(n_1+n_2)/2-1}$  dependence, where  $n_1(n_2)$  is the number of quarks in the initial (final) state. For pion electroproduction on the deuteron (at relatively large momentum transfer and small excitation energies, where the electroproduction process is determined by the inelastic electromagnetic current,  $\gamma^* + d \rightarrow d + \pi^0$ , with  $n_1 = 6$  and  $n_2 = 6 + 2 = 8$ ) we expect a value of  $n_1 + n_2 = 14$ , which corresponds to a steeper decrease of the cross section, compared to elastic  $ed$ -scattering, where  $n_1 + n_2 = 12$ .

The  $Q^2$ -behavior for coherent inelastic deuteron cross section is illustrated in Fig. 8, where we show the results of the parametrization:

$$\sigma_{d\pi^0}(Q^2) = \frac{\sigma_{d\pi^0}(0)}{\left(1 + \frac{Q^2}{m^2}\right)^N}, \quad (6)$$

for  $N = 14$  (dotted line), and for  $m^2=1.41$  GeV<sup>2</sup>, according to [1].

The results from these two approaches are consistent with the present data. As for elastic  $ed$ -scattering [2], the measurement of the cross section alone does not allow us to disentangle predictions given from different models of the deuteron structure.

## V. CONCLUSIONS

Coherent  $\pi^0$  electroproduction on the deuteron,  $e + d \rightarrow e + d + \pi^0$ , at relatively large momentum transfer, has been detected for the first time. The specific conditions of this experiment covered coherent  $\pi^0$ -production in the near threshold region and in the region of excitation of the  $\Delta$ -resonance. A steep decrease with  $Q^2$  of the counting rate has been observed at different values of  $W$ .

The present results show that it is possible to foresee a research programme based on the experimental study of coherent pion electroproduction on the deuteron at relatively large momentum transfer, at threshold and in the  $\Delta$ -region, to access:

- the relative contributions of  $S$ - and  $P$ -waves for different values of  $Q^2$ ,
- the  $Q^2$ -scaling behavior of  $S$ - and  $P$ -waves excitation for  $\gamma^* + d \rightarrow d + \pi^0$ ,
- the specific mass parameter,  $m^2$ , which enters in the  $Q^2$  dependence of the different contributions to the differential cross section to be compared to meson and nucleon form factors values, and
- the  $\Delta$ -isobar excitation on the deuteron,  $\gamma^* + d \rightarrow \Delta + N \rightarrow d + \pi^0$ .

We have established the feasibility of such an experimental study, since counting rates are similar to elastic scattering. More complete results could be obtained at the Jefferson Laboratory in a dedicated experiment, which would stimulate parallel efforts from the theoretical side in developing specific calculations adapted to this newly accessible region. In particular, in addition to differential cross section, measurements of the vector and tensor polarization of the outgoing deuteron are possible in this energy domain [19].

Finally, we would like to recall that after several decades of experimental and theoretical studies of  $ed$  elastic scattering, the situation with the deuteron models (choices of nucleon form factors, deuteron wave functions, corrections to impulse approximation...) is not yet disentangled. In this respect a detailed study of  $e + d \rightarrow e + d + \pi^0$  will bring new important pieces of information.

## VI. ACKNOWLEDGMENTS

We would like to thank all the members of the  $t_{20}$  collaboration for help in taking the data, and, in particular, J. Arvieux, E. Beise, R. Gilman, C. Glashauser and S. Kox, for useful discussions.

## VII. APPENDIX

We present here a possible scheme for the analysis of  $e^- + d \rightarrow e^- + d + \pi^0$  data, taking into account the case of partial information of the detected particles.

For the estimation of the  $\phi$ -acceptance it is necessary to know the relative angle between the 3-momentum of the virtual photon,  $\vec{k}_\gamma$ , and the momentum of the scattered deuteron. This angle depends on the variable  $W$  and can be calculated using the following expression for the production angle of the virtual photon,  $\theta_\gamma$ , relative to the electron scattering angle:

$$\cos \theta_\gamma = \frac{E_2 \cos \theta_e + E_1}{k_\gamma}.$$

### Limited $\phi$ -acceptance

If we approximate the  $\phi$ -acceptance for the emitted deuteron as:

$$-\frac{\Delta\phi}{2} \leq \phi \leq \frac{\Delta\phi}{2},$$

then, for  $\Delta\phi \ll 1$ , all possible contributions in Eq. (2), namely 1,  $\cos 2\phi$  and  $\cos \phi$ , will give the same results:

$$\int_{-\Delta\phi/2}^{\Delta\phi/2} 1 d\phi = \Delta\phi,$$

$$\int_{-\Delta\phi/2}^{\Delta\phi/2} \cos 2\phi d\phi = \sin \Delta\phi \simeq \Delta\phi,$$

$$\int_{-\Delta\phi/2}^{\Delta\phi/2} \cos \phi d\phi = \sin \Delta\phi \simeq \Delta\phi.$$

So we can write the  $\phi$ -integrated cross section as follows:

$$\frac{d^4\sigma}{dE_2 d\Omega d\cos\tilde{\theta}_\pi} = \Delta\phi \mathcal{N} \sigma(Q^2, W, \cos\tilde{\theta}_\pi, E_1),$$

with the following dependence for  $\cos\tilde{\theta}_\pi$ :

$$\sigma(Q^2, W, \cos\tilde{\theta}_\pi, E_1) = A_0 + A_1 \cos\tilde{\theta}_\pi + A_2 \cos^2\tilde{\theta}_\pi + A_3 \sin\tilde{\theta}_\pi + A_4 \sin\tilde{\theta}_\pi \cos\tilde{\theta}_\pi, \quad (7)$$

where the five coefficients  $A_i$  are definite linear combinations of the coefficients (5):

$$\begin{aligned} A_0 &= a_0 + \epsilon(c_0 + b_0), \\ A_1 &= a_1 + \epsilon c_1, \\ A_2 &= a_2 + \epsilon(c_2 - b_0), \\ A_3 &= \sqrt{2\epsilon(1+\epsilon)} d_0, \\ A_4 &= \sqrt{2\epsilon(1+\epsilon)} d_1. \end{aligned} \quad (8)$$

The  $E_1$ -dependence of all these coefficients  $A_i$  is contained only in the parameter  $\epsilon$ .

If we can measure the cross section  $\frac{d^4\sigma}{dE_2 d\Omega d\cos\tilde{\theta}_\pi}$  at five different values of  $\tilde{\theta}_\pi$ , we will determine all the five coefficients  $A_i(Q^2, W, \cos\tilde{\theta}_\pi, E_1)$ , which can be compared to theoretical predictions.

### Full $2\pi$ acceptance

In this case only the L and T components of the cross section contribute to the integral of (2) in the interval  $0 \leq \phi \leq 2\pi$ :

$$\frac{d^4\sigma}{dE_2 d\Omega d\cos\tilde{\theta}_\pi} = 2\pi \mathcal{N} \sigma(Q^2, W, \cos\tilde{\theta}_\pi, E_1),$$

with the following dependence for  $\cos\tilde{\theta}_\pi$ :

$$\sigma(Q^2, W, \cos \tilde{\theta}_\pi, E_1) = A_0 + A_1 \cos \tilde{\theta}_\pi + A_2 \cos^2 \tilde{\theta}_\pi \quad (9)$$

and the three coefficients  $A_i$  are definite linear combinations of the coefficients (5):

$$\begin{aligned} A_0 &= a_0 + \epsilon c_0, \\ A_1 &= a_1 + \epsilon c_1, \\ A_2 &= a_2 + \epsilon c_2. \end{aligned} \quad (10)$$

The Rosenbluth fit in  $\epsilon$  is very useful for the separation of the different contributions to the coefficients  $A_0 - A_2$ .

### A. $\cos \tilde{\theta}_\pi$ -integration

This integration has to be done, if the deuteron energy (in the LAB-system) is not properly measured.

The representation (5) is well adapted to  $\cos \tilde{\theta}_\pi$ -integration over the energy acceptance of the deuteron channel. We can use the one-to-one correspondance between the deuteron energy  $E_d$  (in LAB-system) and  $\cos \tilde{\theta}_\pi$ . From Eq. (2) we find:

$$\cos \tilde{\theta}_\pi = \frac{T_0 - E_d}{T_1},$$

where  $T_0$  and  $T_1$  are:

$$\begin{aligned} T_0 &= \frac{1}{4M} \left[ W^2 - Q^2 - m_\pi^2 + \frac{(M^2 - Q^2)(M^2 - m_\pi^2)}{W^2} \right], \\ T_1 &= \frac{1}{M} \left[ \left( \frac{(W^2 + Q^2 - M^2)^2}{4W^2} - Q^2 \right) \left( \frac{(W^2 + m_\pi^2 - M^2)^2}{4W^2} - m_\pi^2 \right) \right]^{1/2}, \end{aligned}$$

i.e. the energies  $T_0$  and  $T_1$  are functions of  $Q^2$  and  $W$  only.

The final result can be written as:

$$\frac{d^3\sigma}{dE_2 d\Omega} = \Delta\phi \mathcal{N} \tilde{\sigma}(Q^2, W, E_1),$$

where

$$\tilde{\sigma}(Q^2, W, E_1) = A_0 I_0 + A_1 I_1 + A_2 I_2 + A_3 I_3 + A_4 I_4.$$

The coefficients  $I_0 - I_4$  are the integrals over the acceptance of the deuteron channel:

$$\begin{aligned}
I_0 &= \int_{\Delta} d \cos \tilde{\theta}_{\pi} = \frac{1}{T_1} \int_{E_{d,min}}^{E_{d,max}} dE_d, \\
I_1 &= \int_{\Delta} \cos \tilde{\theta}_{\pi} d \cos \tilde{\theta}_{\pi} = -\frac{1}{T_1^2} \int_{E_{d,min}}^{E_{d,max}} (T_0 - E_d) dE_d, \\
I_2 &= \int_{\Delta} \cos^2 \tilde{\theta}_{\pi} d \cos \tilde{\theta}_{\pi} = -\frac{1}{T_1^3} \int_{E_{d,min}}^{E_{d,max}} (T_0 - E_d)^2 dE_d, \\
I_3 &= \int_{\Delta} \sin \tilde{\theta}_{\pi} d \cos \tilde{\theta}_{\pi} = -\frac{1}{T_1} \int_{E_{d,min}}^{E_{d,max}} dE_d \sqrt{1 - \frac{(T_0 - E_d)^2}{T_1^2}}, \\
I_4 &= \int_{\Delta} \sin \tilde{\theta}_{\pi} \cos \tilde{\theta}_{\pi} d \cos \tilde{\theta}_{\pi} = -\frac{1}{T_1^2} \int_{E_{d,min}}^{E_{d,max}} dE_d (T_0 - T_1) \sqrt{1 - \frac{(T_0 - E_d)^2}{T_1^2}},
\end{aligned} \tag{11}$$

where  $E_{d,min}$  and  $E_{d,max}$  are the minimal and maximal energies of the deuteron (in the LAB-system). The coefficients  $I_0 - I_4$  are functions of  $Q^2$  and  $W$ , for each initial energy of the electron beam,  $E_1$ .

The calculation of the coefficients  $A_0 - A_4$ , in the framework of a definite model for  $\gamma^* + d \rightarrow d + \pi^0$ , together with numerical values for  $I_0 - I_4$ , allows a straightforward comparison of the measured cross section  $\frac{d^2\tilde{\sigma}}{dQ^2 dW}$  with theoretical predictions.



## REFERENCES

- [1] S.J. Brodsky and G.R. Farrar, Phys. Rev. Lett. **31**, 1153 (1973);  
S. J. Brodsky and B. T. Chertok, Phys. Rev. D **14**, 3003 (1976);  
Phys. Rev. Lett. **37**, 269 (1976).
- [2] L. C. Alexa *et al.*, Phys. Rev. Lett. **82**, 1374 (1999).
- [3] D. Abbott *et al.*, Phys. Rev. Lett. **84**, 5053 (2000);  
K. Hafidi, PhD thesis, University of Paris XI (1999), France, Report DAPNIA/SPhN-99-05T;  
W. Zhao, PhD thesis, MIT, (1999);  
K. Gustafsson, PhD thesis, University of Maryland, (2000).
- [4] F. Gross and R. Gilman, arXiv:nucl-th/0110015.
- [5] M. Fuchs *et al.*, Phys. Lett. B **368**, 20 (1996);  
A. M. Bernstein, E. Shuster, R. Beck, M. Fuchs, B. Krusche, H. Merkel and H. Stroher,  
Phys. Rev. C **55**, 1509 (1997).
- [6] J.C. Bergström *et al.*, Phys. Rev. C **53**, R1052 (1996)  
J. C. Bergström, R. Igarashi and J. M. Vogt, Phys. Rev. C **55**, 2016 (1997).
- [7] H. B. van der Brink *et al.*, Nucl. Phys. A **612** (1997) 391.
- [8] J. C. Bergström *et al.*, Phys. Rev. C **57**, 3203 (1998).
- [9] M. O. Distler *et al.*, Phys. Rev. Lett. **80**, 2294 (1998);  
I. Ewald *et al.*, Phys. Lett. B **499**, 238 (2001).
- [10] M. P. Rekaló, E. Tomasi-Gustafsson, and J. Arvieux, LNS/Ph/97-20; Ann. of Phys. (NY) **295**, 1 (2002).
- [11] D. G. Meekins *et al.*, Phys. Rev. C **60**, 052201 (1999).
- [12] C. W. Bochna *et al.*, Phys. Rev. Lett. **81**, 4576 (1998);

- E. C. Schulte *et al.*, Phys. Rev. Lett. **86**, 2975 (2001);  
K. Wijesooriya *et al.*, Phys. Rev. Lett. **87**, 102302 (2001).
- [13] M. P. Rekaló and E. Tomasi-Gustafsson, Phys. Rev. C **66**, 015203 (2002).
- [14] A. Akhiezer, M. P. Rekaló, Hadron Electrodynamics, Naukova Dumka, Kiev 1977.
- [15] S. Kox *et al.* Nucl. Instr. Meth. **A346**, 527 (1994);  
S. Real, PhD thesis, University of Grenoble 1 (1994), Report No. ISN-94-04;  
L. Eyraud, PhD Thesis, University of Grenoble 1 (1998), Report No. ISN-98-101.
- [16] D. Abbott *et al.*, Phys. Rev. Lett. **82**, 1379 (1999);  
A. Honegger, PhD thesis, Univ. Basel, Switzerland, (1999);  
D. Pitz, PhD thesis, University of Paris XI (2000), France, Report DAPNIA/SPhN-99-05T.
- [17] D. Pitz,  $T_{20}$  Collaboration Int. Report, 25/2/1999 and private communication.
- [18] V. A. Matveev, R. M. Muradian and A. N. Tavkhelidze, Lett. Nuovo Cim. **7**, 719 (1973).
- [19] E. Tomasi-Gustafsson *et al.*, Nucl. Instrum. Meth. A **420**, 90 (1999).

FIGURES

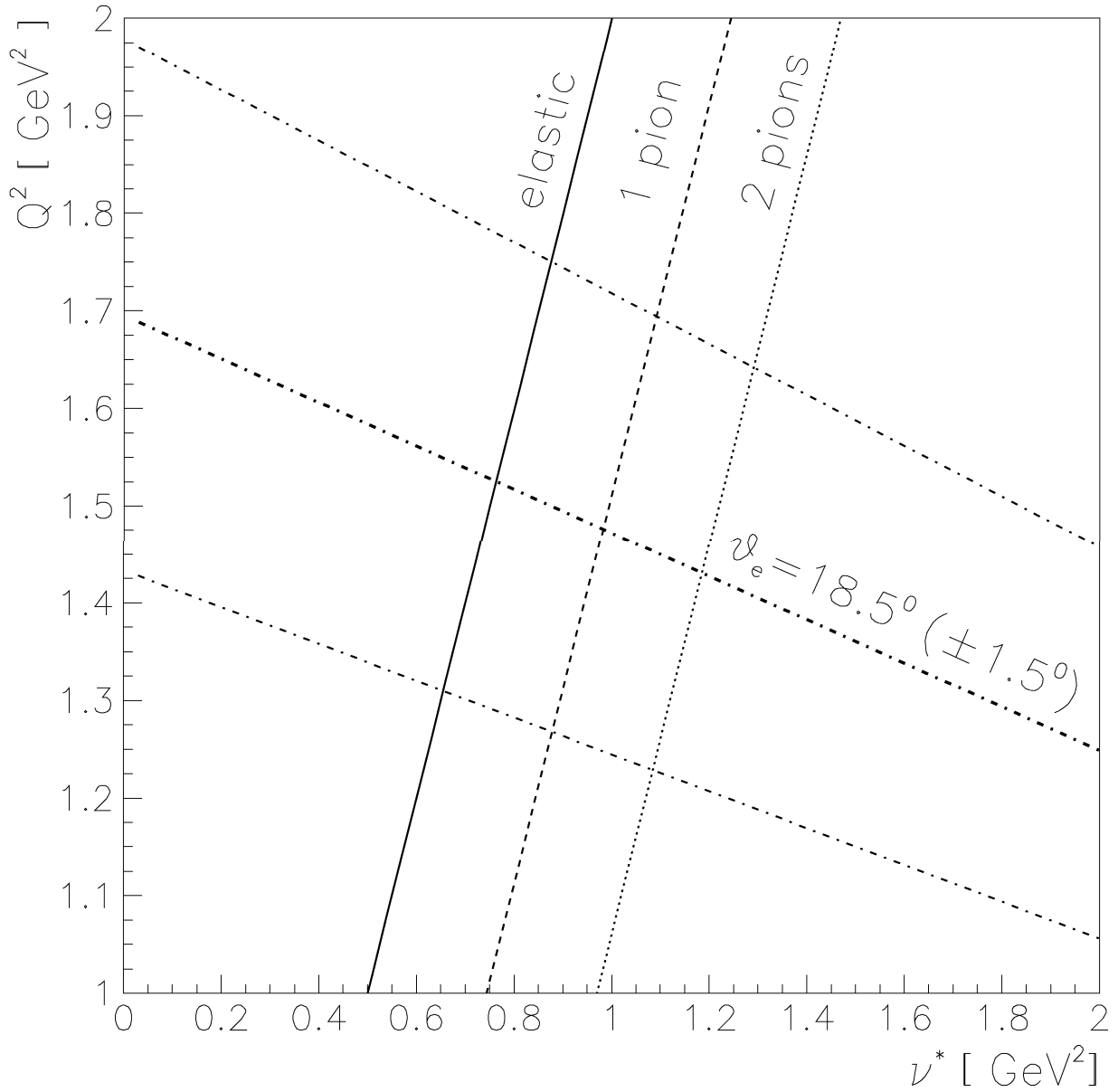


FIG. 1. Kinematical lines of  $ed$ -interaction, in the  $Q^2$  versus  $\nu^*$  plane, calculated for a beam energy  $E_1=4.05$  GeV. The elastic line (solid line) and the threshold lines for one pion (dashed line) and two pion production (dotted line) are indicated. The angular range covered by the kinematics of the electron is also indicated (dashed-dotted lines).

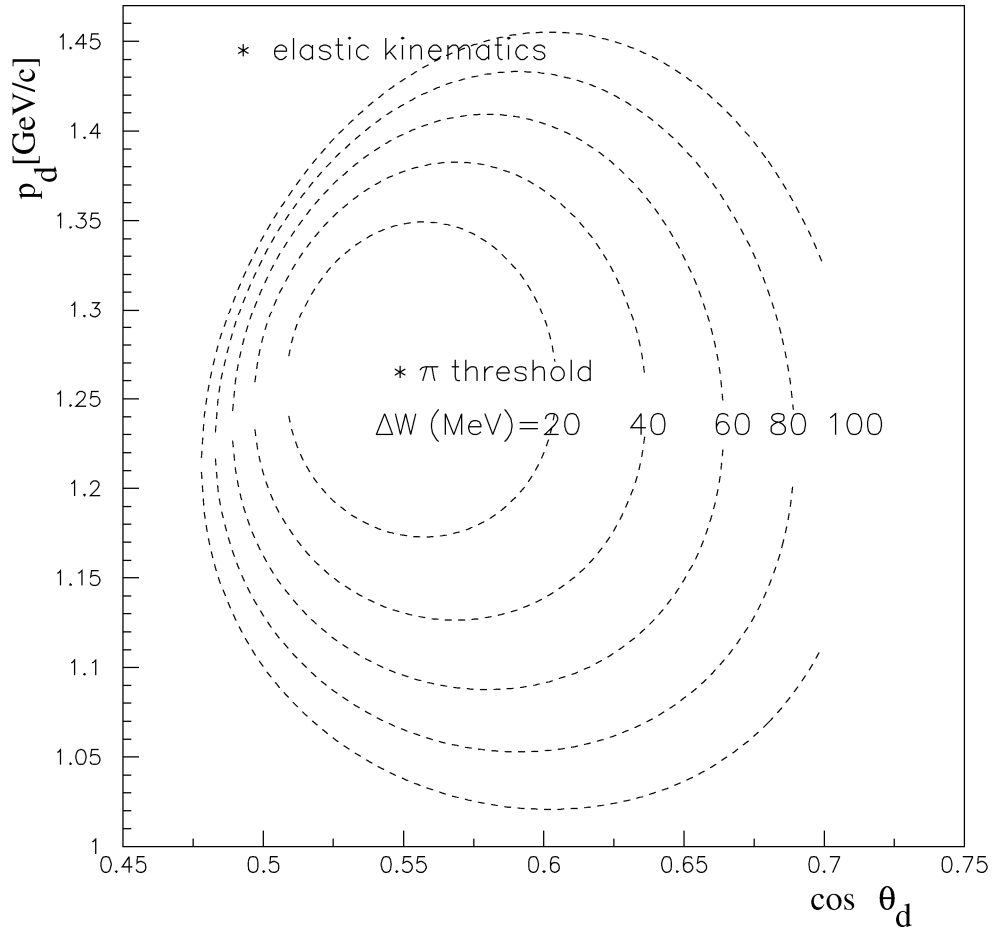


FIG. 2. The deuteron momentum as a function of the deuteron scattering angle, in coplanar kinematics, for different values of  $\Delta W$ , the excess of invariant  $d\pi$ -mass over the pion production threshold. The initial electron energy is  $E_1 = 4.05$  GeV and  $\theta_e = 18.5^\circ$ .

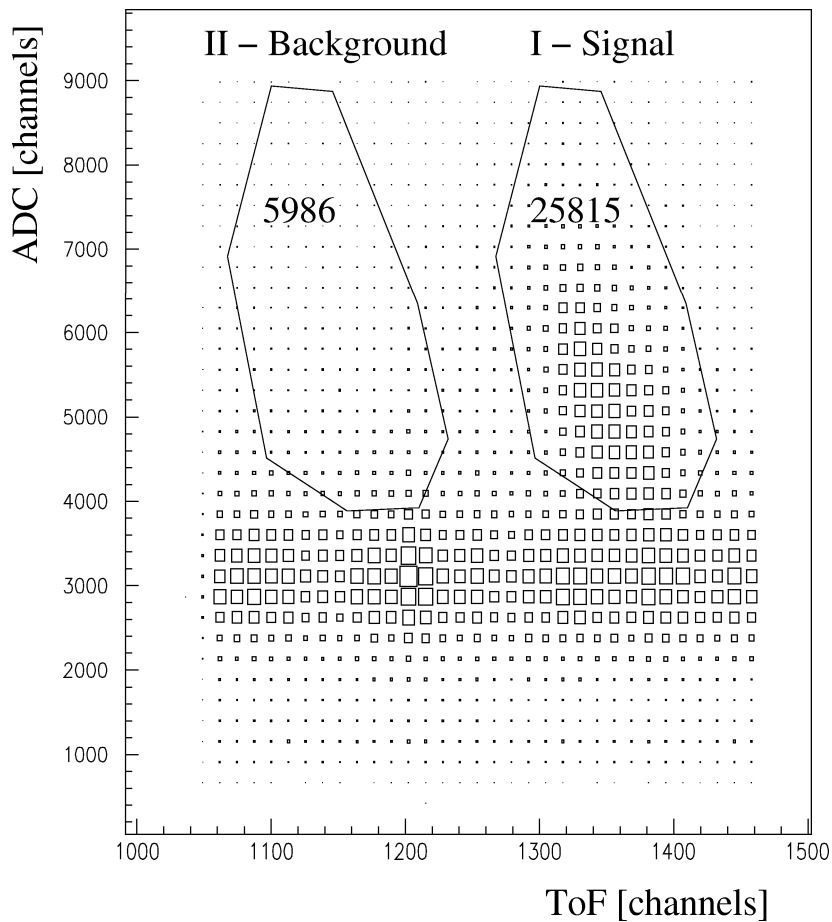


FIG. 3. Two-dimensional plot of the events in the ADC versus time of flight plane. The contours are used to select the deuterons from  $e + d \rightarrow e + d + \pi^0$  events (contour I, labelled 'signal') and to estimate the background (contour II, labelled 'background'). The events at ADC values around 3000 correspond to random electron-protons coincidences.

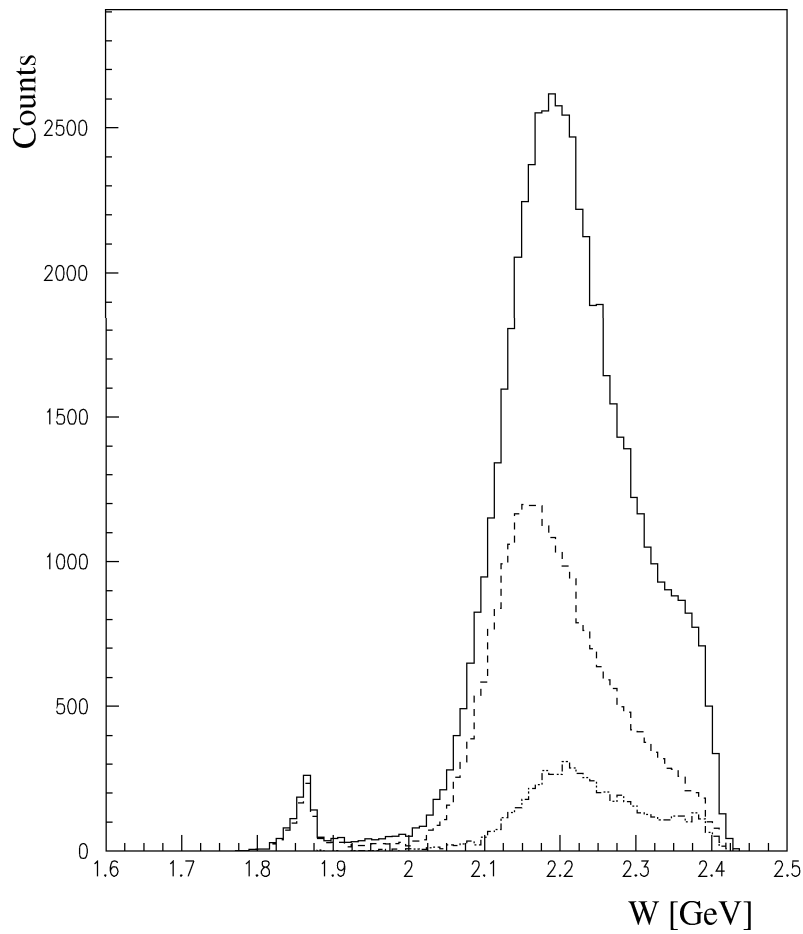


FIG. 4. Experimental distribution of the invariant mass,  $W$ , corresponding to events in the range of time of flight 1280-1440 (full line) and to events selected, according to Fig. 3, by contour I (dashed line) or by contour II (dotted line).

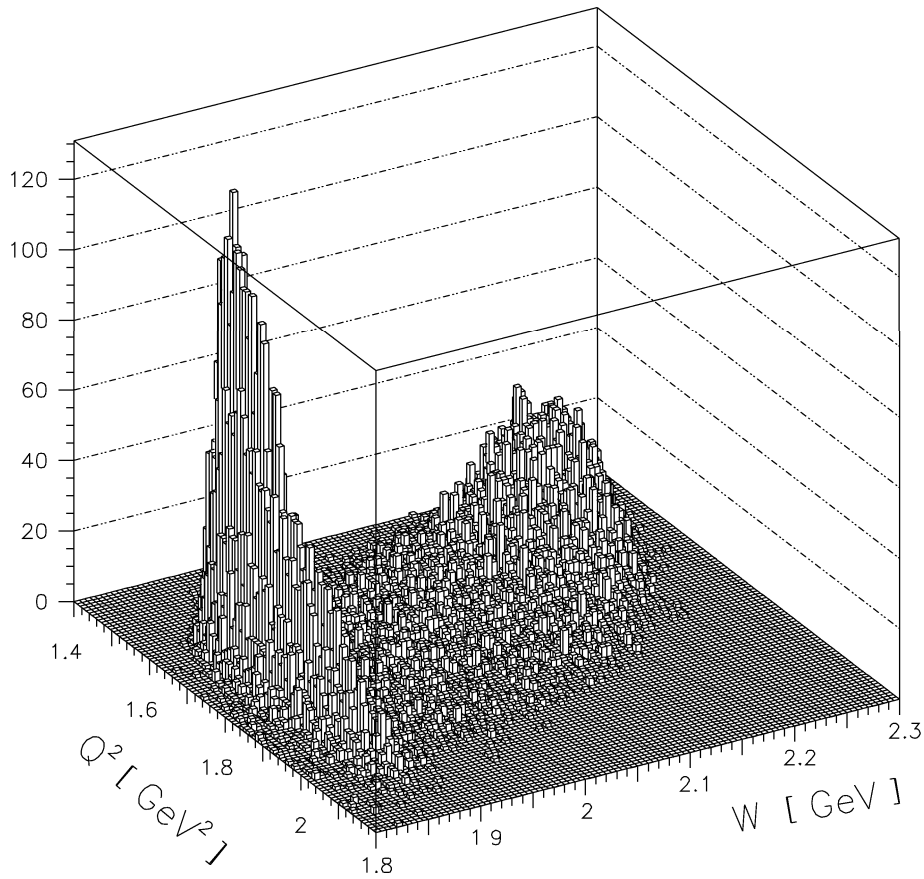


FIG. 5. Two-dimensional plot of the number of counts as a function of momentum transfer squared,  $Q^2$ , and invariant mass of the hadronic system,  $W$ , for the  $e + d \rightarrow e + X$  reaction, in the near elastic kinematics. The beam energy is 4.05 GeV and the  $\theta_e = 20.3^\circ$ . Events corresponding to the elastic peak are centered around  $W = M$ .

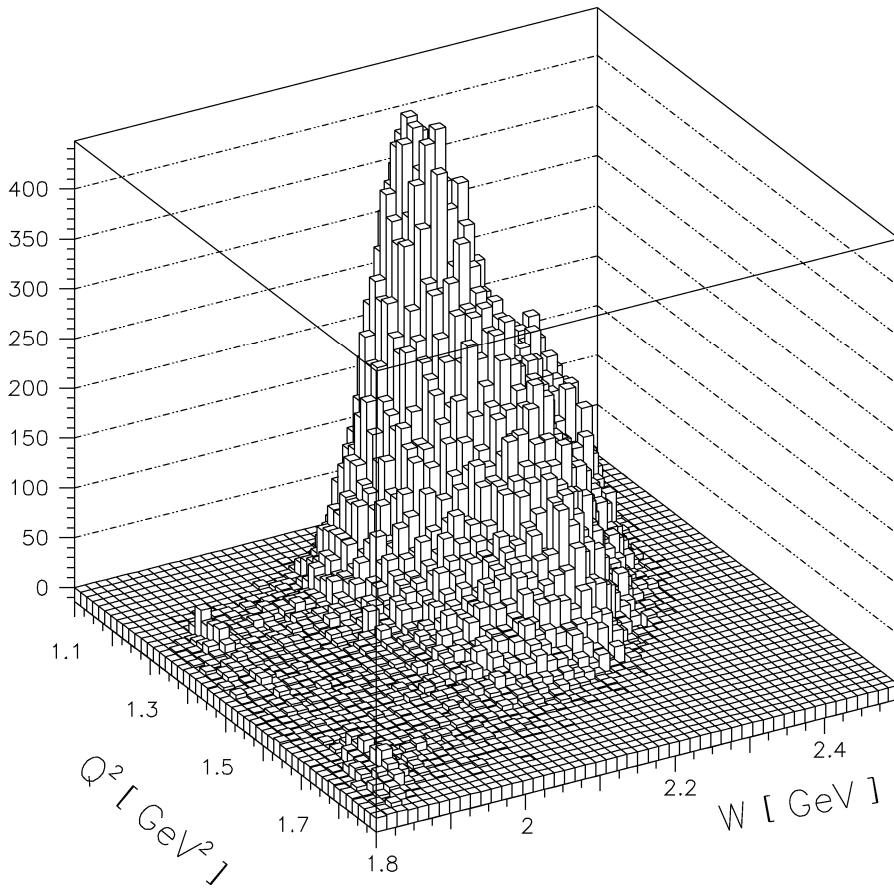


FIG. 6. Two-dimensional plot of the number of counts as a function of momentum transfer,  $Q^2$ , and invariant mass of the hadronic system,  $W$ , for the  $e + d \rightarrow e + X$  reaction, in the pion kinematics. The beam energy is 4.05 GeV and  $\theta_e = 18.5^\circ$ . Events corresponding to pion production are visible for  $W > M + m_\pi$ .



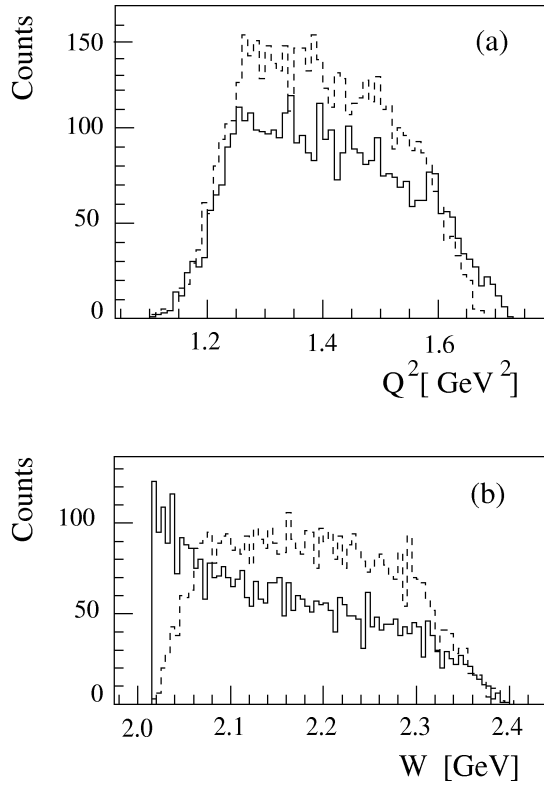


FIG. 7.  $Q^2$ -distribution (a) and  $W$ -distribution (b), following a Monte Carlo simulation. The full line corresponds to an uniform input cross section and the dashed line corresponds to an input distribution corrected by the kinematical factor  $\mathcal{N}$  (Eq. 3).

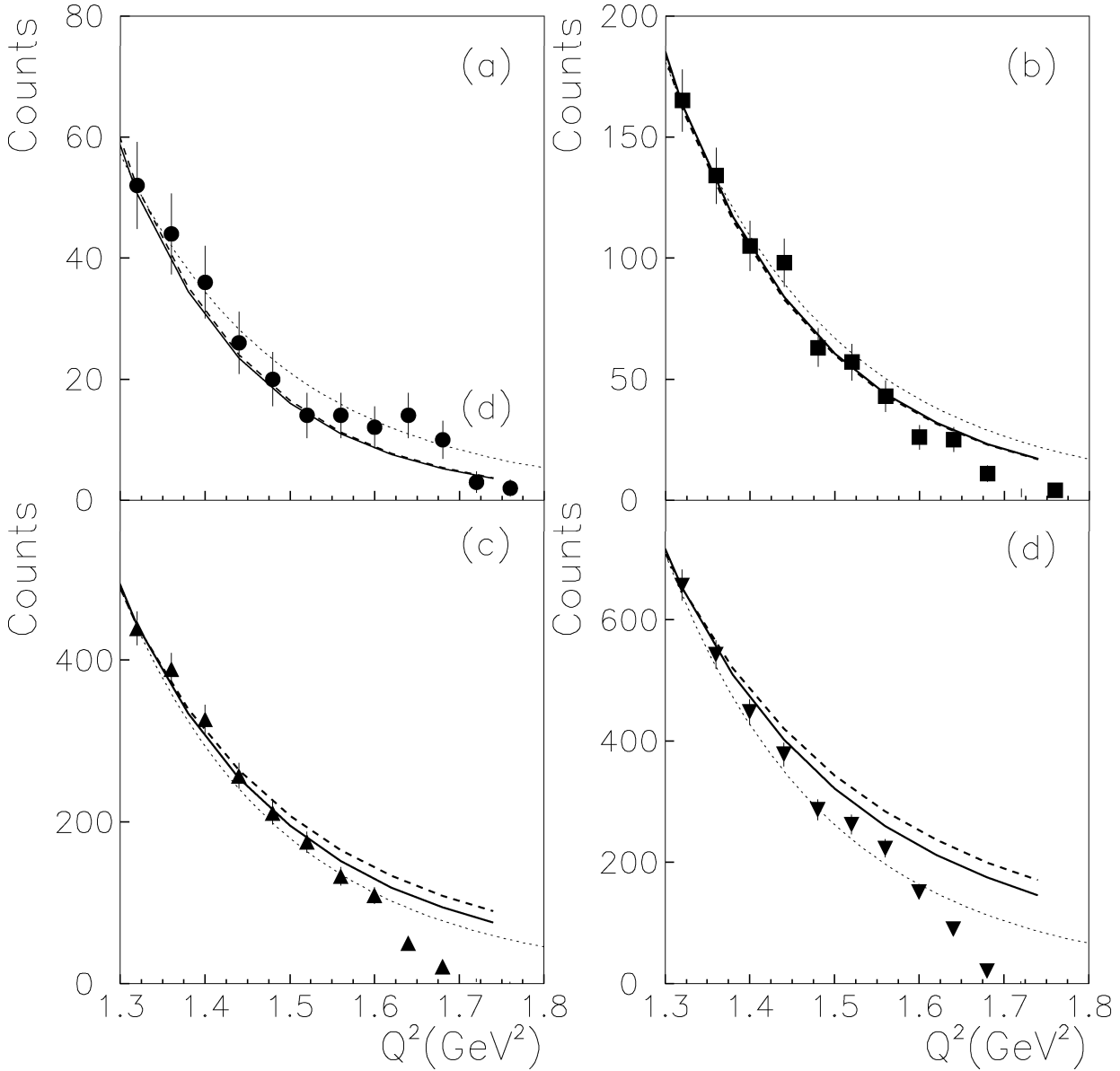


FIG. 8.  $Q^2$ -dependence of the counting rates, corrected by the kinematical factor  $\mathcal{N}$ , see Eq. (3), for different bins of the invariant mass excess  $\Delta W = W - W_{th}$ :  $0 \leq \Delta W \leq 40$  MeV (a);  $40 \text{ MeV} \leq \Delta W \leq 80$  MeV (b);  $80 \text{ MeV} \leq \Delta W \leq 120$  MeV (c);  $120 \text{ MeV} \leq \Delta W \leq 160$  MeV (d). The solid line and dashed lines correspond to different ranges of  $\phi$ -integration, from [10]. The dotted line is the pQCD prediction, with  $N=14$  and  $m^2=1.41 \text{ GeV}^2$  see Eq. (6). All curves are normalized to data at  $Q^2=1.3 \text{ GeV}^2$ .